University of Siena
Department of Information Engineering
Via Roma 56
53100 Siena, Italy

Delft University of Technology
EEMCS - Telecommunication Department
Mekelweg 4
2628 CD, Delft, The Netherlands

Development of Iterative Physical Optics Tools for the Extreme Speed Analysis and Design Techniques for Elliptical Dielectric Lens Antennas

Scientific Report on the Research Activity within the framework of the ESF program entitled "New Frontiers in Millimetre/Sub-Millimetre Waves Integrated Dielectric Focusing Systems"

Author: Giorgio Carluccio
Scientific Advisors: Matteo Albani and Andrea Neto
Date: August 2012

1. Introduction

Millimeter and submillimeter wave systems are becoming increasingly important in many scientific applications in areas such as remote sensing, radio astronomy, radar, imaging applications, and communication systems. Receiving and transmitting radio frequency (RF) systems have traditionally been based on waveguide-technology. Modern technologies enable high-level integration of RF devices with electronic circuits directly on dielectric substrate, thus reducing size, weight, and cost of RF systems. The research project is devoted to the development of a technique which allows a systematic analysis and design procedure of elliptical/hemispherical dielectric lens antennas. Such antennas have demonstrated a significant potential for millimeter and submillimeter wave applications, owing to the possibility of integration with electronic components such as detecting diodes, oscillators and mixers [1]–[5]. In addition, the shape of the lens gives a focusing property provided that the eccentricity (for the elliptical lens) or the extension length/radius ratio (for the hemispherical lens) is properly related to the dielectric constant. Under these conditions all the rays leaving a focal source are refracted in the boresight direction, thus providing high directivity to the antennas. Furthermore, lenses provide a good efficiency with respect to other millimeter wave antennas printed on homogeneous substrates, essentially because they do not suffer from loss of power in guided modes [1]–[5]. The use of dielectric lenses in future space science missions [4] requires to host, in the lens focal plane, a large integrated array that can be used efficiently over very wide frequency bands [5].

Due to the large dimensions of the lens in terms of the wavelength, to the large number of radiating elements of the array, and to the large number of simulations, that are necessary for the analysis and the design of the entire radiating system (the integrated array together with the lens), the use of a complete full-wave analysis is impractical, since very time-consuming. For these reasons, the aim of the research project was to develop a numerically efficient Physical Optics (PO) based algorithm to investigate the lens radiation properties.

2. Description of the Developed Physical Optics Efficient Numerical Integration Algorithm

We consider the field radiated by a single element, located in P', of an integrated array covered by a dielectric lens (Fig. 2.1(a)). Since the lens is large, we assume that the array radiates an unperturbed electromagnetic field $\left(\mathbf{E}^u, \mathbf{H}^u\right)$ as in a semi-infinite medium characterized by the same dielectric constant ε_r of the lens (Fig. 2.1(b)). Each single element radiates an electromagnetic field which has a ray field structure at the lens interface. Under the Geometrical Optics (GO) approximation, the field on the external surface of the lens can be approximated by the GO transmitted field $\left(\mathbf{E}^t, \mathbf{H}^t\right)$ (Fig. 2.1(c)). By applying the equivalence principle at the lens interface (Fig. 2.1(d)), the lens interface is substituted by equivalent electric and magnetic currents $\left(\mathbf{J}_{\text{eq}}, \mathbf{M}_{\text{eq}}\right)$ that radiate in free space the following electromagnetic field

$$\begin{aligned}\mathbf{E}(P) &= jk_0 \iint_S \left[\hat{\mathbf{r}} \times \mathbf{M}_{\text{eq}}(Q) + \zeta_0 \hat{\mathbf{r}} \times \hat{\mathbf{r}} \times \mathbf{J}_{\text{eq}}(Q)\right] \frac{e^{-jk_0 r}}{4\pi r} dS \\ \mathbf{H}(P) &= jk_0 \iint_S \left[\frac{1}{\zeta_0} \hat{\mathbf{r}} \times \hat{\mathbf{r}} \times \mathbf{M}_{\text{eq}}(Q) - \hat{\mathbf{r}} \times \mathbf{J}_{\text{eq}}(Q)\right] \frac{e^{-jk_0 r}}{4\pi r} dS\end{aligned} \tag{2.1}$$

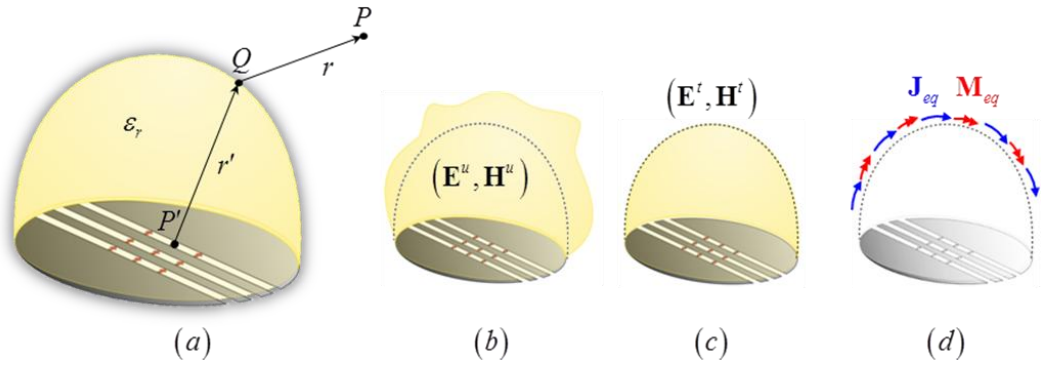

Fig. 2.1. Lens reference geometry and relevant application of the equivalence theorem.

in the far field region of the lens. In (2.1) k_0 and ζ_0 are the wavenumber and the impedance of the free space, respectively; r is the distance between an integration point Q on the lens interface and the observation point P; and $\hat{\mathbf{r}}$ is the unit vector that points from Q to P. Under the GO/PO approximation the equivalent currents can be evaluated as

$$\begin{aligned} \mathbf{J}_{\text{eq}} &\simeq \hat{\mathbf{n}} \times \mathbf{H}^t = \hat{\mathbf{n}} \times \left(\mathbf{H}^i + \mathbf{H}^r \right) \\ \mathbf{M}_{\text{eq}} &\simeq \mathbf{E}^t \times \hat{\mathbf{n}} = \left(\mathbf{E}^i + \mathbf{E}^r \right) \times \hat{\mathbf{n}} \end{aligned} \tag{2.2}$$

where $\hat{\mathbf{n}}$ is the outer pointing normal to the lens interface, and the indexes *i* and *r* identifies the incident and reflected field at the lens interface. By GO assumption, such field contributions can be evaluated by using proper dyadic Fresnel reflection and transmission coefficients defined as in [2], [3], [6]–[8].

As it is well known, the integrals in (2.1) have the following form

$$\mathbf{I} = \iint_D \mathbf{G}(\mathbf{q}) e^{-jk_0 f(\mathbf{q})} du dv = \iint_D \mathbf{F}(\mathbf{q}) du dv \tag{2.3}$$

where $\mathbf{G}(\mathbf{q})$ is a slowly varying function, and $f(\mathbf{q})$ is a phase function, both of which depend on the bidimensional vector $\mathbf{q} \equiv (u, v)$, that parameterizes the integration variables on the domain D, where the parametric surface S of the lens interface is defined. In the literature, various approaches have been proposed to evaluate this kind of integral [9]–[16]. In this work, we specialized one of the integration algorithms presented in [16] to the analysis of the PO radiation from a dielectric lens in order to obtain a new efficient engineering tool for the lens design. In particular, in order to reduce the computational burden, it is important to reduce as much as possible the number of sampling points and to use simple, but accurate, quadrature rule for the evaluation of the radiation integral. Such features have been obtained by using a "quasi equi-spaced" sampling grid, [17], [18], on the lens surfaces, that divides the lens surface into curvilinear triangles (Fig. 2.2), and the quadrature rule in [16] which assumes a linear amplitude and phase approximation of the integrand on each triangles T_m. The integral in (2.3) is than evaluated as the sum of the integrals on all the triangles in which the surface is divided; i.e.,

$$\mathbf{I} = \sum\nolimits_m \mathbf{J}_m, \text{ where } \mathbf{J}_m = \iint_{T_m} \mathbf{F}(\mathbf{q}) du dv. \tag{2.4}$$

By neglecting the index *m* for the sake of readability, the integral on each triangle is evaluated as

$$\mathbf{J} \simeq \sum_{i=1}^{3} \mathbf{F}(\mathbf{v}_i) \iint_T b_i(\mathbf{q}) e^{-jk_0 \mathbf{u}_0 \cdot (\mathbf{q} - \mathbf{v}_i)} du dv = \sum_{i=1}^{3} \mathbf{F}(\mathbf{v}_i) B_i(\mathbf{u}_0), \tag{2.5}$$

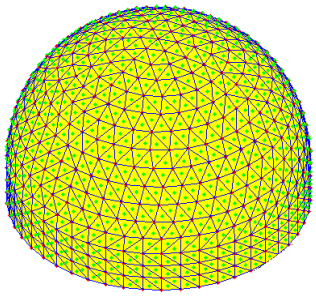

Fig. 2.2. Representative loose curvilinear triangular mesh on the surface of the lens.

where $\mathbf{v}_i$, with $i=1,2,3$, are the bidimensional vectors that identify the vertices of the triangle in the surface parametric domain D; b_i denotes a linear basis function which equals 1 at the ith vertex $\mathbf{v}_i$ and vanishes on the opposite side; and $\mathbf{u}_0$ is the gradient of the phase function at the barycenter of the triangle [16]. The integral $B_i(\mathbf{u}_0)$ is calculated analytically as a Fourier transform, thus obtaining the final closed form expression

$$\begin{aligned} B_i(\mathbf{u}_0) &= \iint_T b_i(\mathbf{q}) e^{-jk_0\mathbf{u}_0\cdot(\mathbf{q}-\mathbf{v}_i)} du dv \\ &= 2S_T \left(\frac{-1}{k_0^2\left[\mathbf{u}_0\cdot(\mathbf{v}_{i+2}-\mathbf{v}_i)\right]\left[\mathbf{u}_0\cdot(\mathbf{v}_{i+1}-\mathbf{v}_i)\right]} + \frac{\mathbf{u}_0\cdot\left[(\mathbf{v}_{i+1}-\mathbf{v}_i)+(\mathbf{v}_{i+2}-\mathbf{v}_i)\right]}{jk_0^3\left[\mathbf{u}_0\cdot(\mathbf{v}_{i+1}-\mathbf{v}_i)\right]^2\left[\mathbf{u}_0\cdot(\mathbf{v}_{i+2}-\mathbf{v}_i)\right]^2} \right. \\ &\left. + \frac{e^{-jk_0\mathbf{u}_0\cdot(\mathbf{v}_{i+2}-\mathbf{v}_i)}}{jk_0^3\mathbf{u}_0\cdot(\mathbf{v}_{i+2}-\mathbf{v}_{i+1})\left[\mathbf{u}_0\cdot(\mathbf{v}_{i+2}-\mathbf{v}_i)\right]^2} + \frac{e^{-jk_0\mathbf{u}_0\cdot(\mathbf{v}_{i+1}-\mathbf{v}_i)}}{jk_0^3\mathbf{u}_0\cdot(\mathbf{v}_{i+1}-\mathbf{v}_{i+2})\left[\mathbf{u}_0\cdot(\mathbf{v}_{i+1}-\mathbf{v}_i)\right]^2} \right), \end{aligned} \tag{2.6}$$

in which S_T is the area of the triangle in the parametric domain. The Fourier transform (2.6) is a regular function at any incidence/observation aspects except for removable singularities; indeed when any of the denominators in (2.6) vanishes, B_i admits a limit which has an analytic closed form expression. Expression (2.5) can be thought of as a surface quadrature rule with sampling points at triangle vertices $\mathbf{v}_i$ and weights $B_i(\mathbf{u}_0)$ depending on the phase progression rate $\mathbf{u}_0$. The use of the vertices as sampling points is convenient because, since the integral in (2.6) presents a linear phase, from an asymptotic point of view the main contributions to the integral come from the vertices. Thus, for the accurate evaluation of the integral $\mathbf{I}$, it is very important to match the integrand of $\mathbf{J}$ at these critical points.

The proposed algorithm has to be applied iteratively for each radiating element of the integrated array. The total radiated field from the lens is obtained as the sum of all the field contributions arising from each single array element.

3. Numerical Results

To validate the behaviour of the proposed algorithm we applied it to the analysis of the following device. We considered a square array of 3x3 connected slots [5] which radiates in the presence of a hemispherical dielectric lens with relative dielectric constant $\varepsilon_r = 11.7$, radius $R = 95\text{mm}$, and extension length $L_{ext} = 0.3R$. The central element of the array is in the equivalent focus of the hemispherical lens. We consider an operating frequency of $f = 5\text{GHz}$ and $f = 15\text{GHz}$ in the first and second example, respectively. The developed code was tested on an Intel i7-720QM

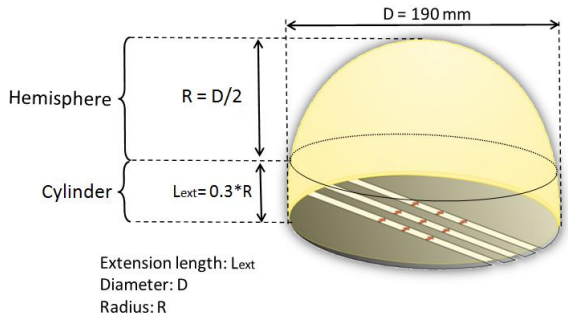

Fig. 3.1. Lens reference examples geometry.

Table 1

Triangle Side Length	Number of Triangles	Computational Time
Example 1		
$\lambda/5$	834	19s
$\lambda/10$	3190	60s
$\lambda/15$	7262	135s
Example 2		
$\lambda/5$	7262	190s
$\lambda/10$	28577	700s

processor with a clock frequency of 1.6GHz (turbo up to 2.8GHz), Cache and RAM memory of 6MB and 6GB, respectively. Table 1 resumes the algorithm performances for both the examples by varying the length of the triangle sides in the various meshes (first column). The second column of the table contains the number of triangles created by the meshing process, while the third column contains the computational time necessary for the field evaluation along the scans in the lens azimuthal plane $\phi = 0°$, $\phi = 45°$, and $\phi = 90°$, when a single element of the array is fed. In the first example ($f = 5\text{GHz}$) we test the behaviour of the algorithm with three different meshes by varying the length of the triangle side; namely, $\lambda/15$, $\lambda/10$, and $\lambda/5$. Fig. 3.2 shows the normalized radiation patterns obtained. In particular, the patterns in Fig. 3.2(a) are those obtained when the central element of the array is fed, while the patterns in Fig. 3.2(b) are those obtained when the first off-focus element, in the *y* direction of the $x = 0$ plane of the array, is fed. Such figure shows that a mesh where the side of triangles is about $\lambda/10$ is sufficient to obtain an accurate result. Indeed, the lines associated to the patterns obtained by the mesh with triangle sides of about $\lambda/10$ are superimposed to those obtained by the mesh with triangle sides of about $\lambda/15$. However, accurate results (till to 20 dB respect to the maximum value of the pattern) can be obtained with a coarser mesh; i.e., a mesh where the side of triangles is about $\lambda/5$, thus obtaining a reduction of the computational time (Table 1). The same behaviour is also observed in the second example ($f = 15\text{GHz}$), where we used two different kind of meshes with the length of the triangle side of about $\lambda/10$ and $\lambda/5$. Fig. 3.3(a) shows the patterns obtained when the central element of the array is fed, while the patterns in Fig. 3.3(b) are those obtained when the first off-focus element, in the *y* direction of the $x = 0$ plane of the array, is fed. Also in this case, accurate results can be obtained with a mesh where the side of triangles is about $\lambda/5$, thus again obtaining a reduction of the computational time (Table 1).

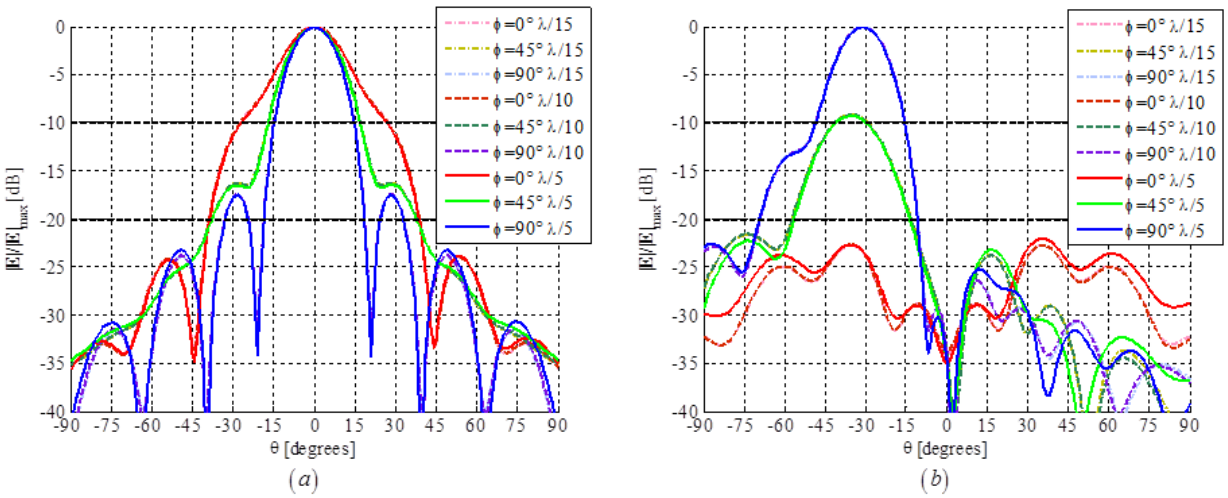

Fig. 3.2. Lens radiation patterns obtained with different length of triangle sides in the mesh. (a) The patterns are those obtained when the central element of the array is fed. (b) The patterns are those obtained when the first off-focus element, in the *y* direction of the x=0 plane of the array, is fed.

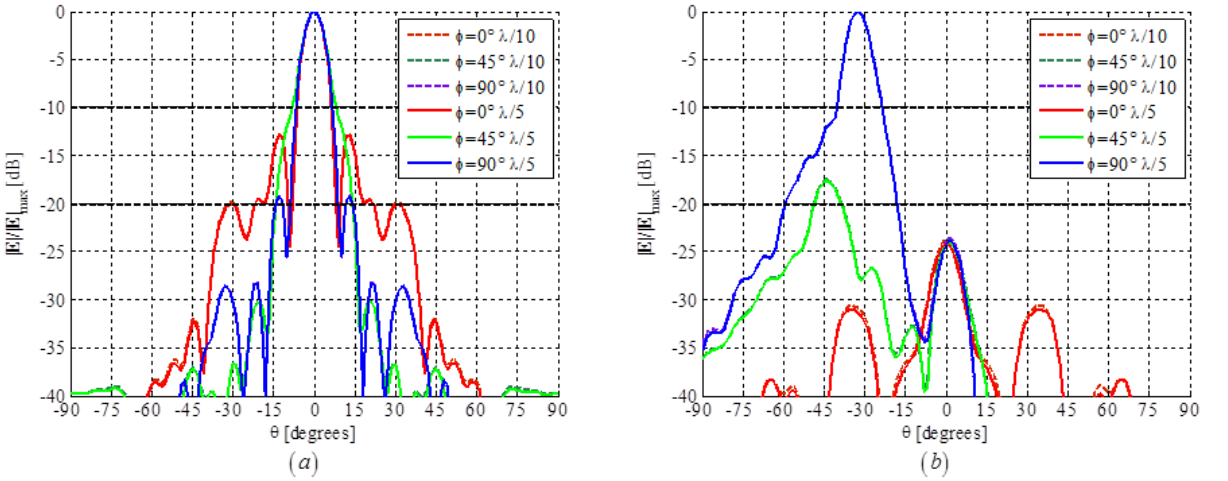

Fig. 3.3. Lens radiation patterns obtained with different length of triangle sides in the mesh. (a) The patterns are those obtained when the central element of the array is fed. (b) The patterns are those obtained when the first off-focus element, in the *y* direction of the x=0 plane of the array, is fed.

4. Concluding Remarks

In the framework of NEWFOCUS research programme we developed an efficient algorithm for the calculation of the field radiated from a dielectric lens antenna under PO approximation. By this algorithm the numerical evaluation of the PO radiation integral is performed on the lens surface parametric domain. The original integration domain is divided into triangular sub-domains, whose mapping on the surface gives curvilinear triangles that are "quasi equi-area". On each triangular sub-domain both the amplitude and the phase of the integrand are linearly approximated and the relevant integral is analytically evaluated in closed form. The proposed algorithm was applied to some preliminary tests for analyzing the scattering of the lens when its interface is illuminated by an element of an array of connected

slots. The presented examples show that the developed algorithm reaches accurate results also when the mesh on the lens has loose samples.

This work was presented at 2012 IEEE International Symposium on Antennas and Propagation and USNC-URSI National Radio Science Meeting that was held in July 2012 in Chicago, Illinois, USA, [19], and will also be object of future publications on scientific journals. This algorithm was also used to obtain some results presented in [20] and [21] during the same conference. Finally, the proposed algorithm will be iteratively used for the design optimization of large lenses illuminated by arrays formed by a large number of radiating elements. At the Technical University of Delft a first prototype of an array of connected slots covered by a hemispherical dielectric lens with the same features presented in the examples of this report has been built (Fig. 4.1). Its radiating features will be measured and a comparison against the results obtained by the described algorithm will be performed. Such activity could also be realized in the framework of NEWFOCUS programme.

Fig. 4.1. Hemispherical dielectric lens fed by an array of connected slots built at the Technical University of Delft.

5. References

[1] G. M. Rebeiz, "Millimeter-wave and terahertz integrated circuit antennas," *Proc. IEEE*, vol. 80, no. 11, pp. 1748–1770, Nov. 1992.

[2] D. F. Filipovic, S. S. Gearhart, and G. M. Rebeiz, "Double-slot antennas on extended hemispherical and elliptical silicon dielectric lenses," *IEEE Trans. Microwave Theory Tech.*, vol. 41, no. 10, pp. 1738–1749, Oct. 1993.

[3] D. F. Filipovic, G. P. Gauthier, S. Raman, and G. M. Rebeiz, "Off-axis properties of silicon and quartz dielectric lens antennas," *IEEE Trans. Antennas Propag.*, vol. 45, no. 5, pp. 760–766, May 1997.

[4] A. Baryshev, J. J. A. Baselmans, A. Freni, G. Gerini, H. Hoevers, A. Iacono, and A. Neto, "Progress in antenna coupled kinetic inductance detectors," *IEEE Trans. THz Sci. Technol.*, vol. 1, no. 1, pp. 112–123, Sept. 2011.

[5] D. Cavallo and A. Neto, "A connected array of slots supporting broadband leaky waves," submitted to *IEEE Trans. Antennas Propag.*, Aug. 2012.

[6] W. D. Burnside and K. W. Burgener, "High frequency scattering by a thin lossless dielectric slab," *IEEE Trans. Antennas Propag.*, vol. AP-31, no. 1, pp. 104–110, Jan. 1983.

[7] Y. Rahmat-Samii and A. N. Tulintseff, "Diffraction analysis of frequency selective reflector antennas," *IEEE Trans. Antennas Propag.*, vol. 41, no. 4, pp. 476–487, Apr. 1993.

[8] M. Albani, G. Carluccio and P. H. Pathak, "Uniform ray description for the PO scattering by vertices in curved surface with curvilinear edges and relatively general boundary conditions," *IEEE Trans. Antennas Propag.*, vol. 59, no. 5, pp. 1587–1596, May 2011.

[9] A. C. Ludwig, "Computation of radiation patterns involving numerical double integration," *IEEE Trans. Antennas Propag.*, vol. 16, no. 6, pp. 767–769, Nov. 1968.

[10] W. B. Gordon, "Far-field approximations to the Kirchhoff-Helmholtz representation of scattered fields," *IEEE Trans. Antennas Propag.*, vol. AP-23, no. 4, pp. 590–592, Jul. 1975.

[11] G. Crabtree, "A numerical quadrature technique for physical optics scattering analysis," *IEEE Trans. Magn.*, vol. 27, no. 5, pp. 4291–4294, Sept. 1991.

[12] A. Boag and C. Letrou, "Fast radiation pattern evaluation for lens and reflector antennas", *IEEE Trans. Antennas Propag.*, vol. 51, no. 5, pp. 1063–1068, May 2003.

[13] R. J. Burkholder and T.-H. Lee, "Adaptive sampling for fast physical optics numerical integration," *IEEE Trans. Antennas Propag.*, vol. 53, no. 5, pp. 1843–1845, May 2005.

[14] C. Delgado, J. Gónzalez, and F. Cátedra, "Analytic field calculation involving current modes and quadratic phase expressions," *IEEE Trans. Antennas Propag.*, vol. 55, no. 1, pp. 233–240, Jan. 2007.

[15] F. Vico-Bondia, M. Ferrando-Bataller, and A. Valero-Nogueira, "A new fast physical optics for smooth surfaces by means of a numerical theory of diffraction," *IEEE Trans. Antennas Propag.*, vol. 58, no. 3, pp. 773–789, Mar. 2010.
[16] G. Carluccio and M. Albani, "Efficient adaptive numerical integration algorithms for the evaluation of surface radiation integrals in the high-frequency regime," *Radio Sci.*, Vol. 46, RS0E04, 2011.
[17] P.-S. Kildal, "Synthesis of multireflector antennas by kinematic and dynamic ray tracing," *IEEE Trans. Antennas Propag.*, vol. 38, no. 10, pp. 1587–1599, Oct. 1990.
[18] P.-S. Kildal, "Analysis of numerically specified multireflector antennas by kinematic and dynamic ray tracing," *IEEE Trans. Antennas Propag.*, vol. 38, no. 10, pp. 1600–1606, Oct. 1990.
[19] G. Carluccio, M. Albani, and A. Neto, "An iterative physical optics algorithm for the analysis and design of dielectric lens antennas," 2012 IEEE International Symposium on Antennas and Propagation and USNC-URSI National Radio Science Meeting, Chicago, Illinois, USA, July 8–14, 2012.
[20] G. Fiorentino, W. H. Syed, P. M. Sarro, and A. Neto, "Artificial dielectric layer as sub-mm wave antenna super-strates," 2012 IEEE International Symposium on Antennas and Propagation and USNC-URSI National Radio Science Meeting, Chicago, Illinois, USA, July 8–14, 2012.
[21] A. Neto and D. Cavallo, "Non dispersive antenna array architectures for THz sensing systems: connected leaky wave slots," 2012 IEEE International Symposium on Antennas and Propagation and USNC-URSI National Radio Science Meeting, Chicago, Illinois, USA, July 8–14, 2012.